IOPscience iopscience.iop.org

Home Search Collections Journals About Contact us My IOPscience

Thermal lattice scattering mobility and carrier effective mass in intrinsic $Tl_2InGaTe_4$ single crystals

This article has been downloaded from IOPscience. Please scroll down to see the full text article.

2007 J. Phys.: Condens. Matter 19 156206

(http://iopscience.iop.org/0953-8984/19/15/156206)

View the table of contents for this issue, or go to the journal homepage for more

Download details:
IP Address: 129.252.86.83
The article was downloaded on 28/05/2010 at 17:39

Please note that terms and conditions apply.

J. Phys.: Condens. Matter **19** (2007) 156206 (6pp) doi:10.1088/0953-8984/19/15/156206

Thermal lattice scattering mobility and carrier effective mass in intrinsic $Tl_2InGaTe_4$ single crystals

A F Qasrawi[1,3] and N M Gasanly[2]

[1] Department of Electrical and Electronics Engineering, Atilim University, Ankara 06836, Turkey
[2] Department of Physics, Middle East Technical University, Ankara 06531, Turkey

E-mail: a_qasrawi@atilim.edu.tr

Received 15 December 2006, in final form 14 February 2007
Published 16 March 2007
Online at stacks.iop.org/JPhysCM/19/156206

Abstract
Systematic structural, dark electrical resistivity and Hall coefficient measurements have been carried out on n-type $Tl_2InGaTe_4$ single crystals. The data from x-ray powder diffraction allowed determination of the tetragonal unit cell lattice parameters. Analysis of the electrical resistivity and carrier concentration, which was recorded in the temperature range 210–350 K, reveals the intrinsic type of conduction with an average energy band gap of 0.85 eV. The temperature-dependent Hall mobility was observed to follow the $\mu \propto T^{-3/2}$ law and was analysed assuming the domination of acoustic phonons scattering. The experimental Hall mobility data for $Tl_2InGaTe_4$ crystals agrees with the theoretical acoustic phonon scattering mobility data with an acoustic deformation potential of 7.6 eV.

1. Introduction

Ternary thallium chalcogenide semiconductors of the III–III–VI_2 family have both layered ($TlGaS_2$, $TlGaSe_2$, $TlInS_2$) and chain ($TlInSe_2$, $TlInTe_2$, $TlGaTe_2$) structures [1]. The compound $Tl_2InGaTe_4$ belongs to the group of semiconductors with a chain structure. This crystal is a structural analogue to $TlInTe_2$ ($TlGaTe_2$), in which half of the trivalent indium (gallium) atoms is replaced by gallium (indium) atoms [1]. In the lattice of the $Tl_2InGaTe_4$ crystal, indium (gallium) atoms are each surrounded by four tellurium atoms and form chains along the tetragonal c-axis. These chains are connected to each other by univalent thallium atoms.

Some of the electrical and optical properties of $TlInTe_2$ and $TlGaTe_2$ crystals have been reported [2–11]. In particular, the fundamental absorption edge is reported to be formed by indirect transitions with energies of 0.97–0.99 and 0.84 eV for $TlInTe_2$ and $TlGaTe_2$, respectively [2, 5]. Consistent with that, temperature-dependent electrical conductivity

[3] Author to whom any correspondence should be addressed.

0953-8984/07/156206+06$30.00 © 2007 IOP Publishing Ltd Printed in the UK

measurements revealed that both crystals are intrinsic, with energy band gaps of 0.80 and 0.85 eV, respectively [5–7]. These compounds exhibit many nonlinear effects in their electrical behaviour, such as S-type characteristics with voltage oscillations in the negative resistance region, switching and memory effects [2–4]. One of the most useful properties of $TlInTe_2$ and $TlGaTe_2$ crystals is the high thermoelectric power [8]. It has been reported that in $TlInTe_2$ crystal a continuous semiconductor-to-metal transition is accomplished under a hydrostatic pressure of $P_t = 6$ GPa [9]. A phase transition in $TlGaTe_2$ chain crystals has been revealed at $T = 98.5$ K [10]. Incommensurate phase structural features have been observed. Recently, band structure calculations have also been reported for $TlInTe_2$ and $TlGaTe_2$ chain crystals [12–14]. For the latter crystal, from angle-resolved photoemission study a strong temperature-dependent shift of the Fermi level was ascertained [15].

The main purpose of this work is to study and discuss some of the physical properties of compound $Tl_2InGaTe_4$, which belongs to the above reviewed crystal group. In particular, a physical interpretation of the Hall properties, the carrier effective mass and the dominant scattering mechanism in the crystals will be reported for the first time.

2. Experimental details

Single crystals of $Tl_2InGaTe_4$ were grown by the Bridgman method from a stoichiometric melt of the starting materials sealed in evacuated (10^{-5} Torr) silica tubes with a tip at the bottom. The resulting ingots (grey-black in colour) showed good optical quality and were easily cleaved along two mutually perpendicular planes parallel to the c-axis of the crystal. The x-ray powder diffraction technique was used to identify the crystalline nature of the $Tl_2InGaTe_4$ compound. For this purpose, Philips PW1740 diffractometer with a monochromatic Cu Kα radiation ($\lambda = 0.154\,049$ nm) at a scanning speed of $0.02°\ 2\theta\ s^{-1}$ was used. Typical dimensions of the crystals suitable for measurements were $5 \times 5 \times 2$ mm^3. Using silver paste, four point contacts were fixed on the top surface of the sample. The ohmic nature of the contacts was confirmed from the I–V characteristics. These characteristics, recorded perpendicular to the crystal's c-axis, were found to be linear and independent of the reversal current. Hall coefficient and electrical resistivity data were recorded in a Lake Shore 7507 Hall-effect measurements system at different temperatures. Measurements were performed under magnetic fields of up to 1.4 T, using a 7 inch variable-gap electromagnet, applied perpendicular to the current direction. Hall-effect data were collected using an IEEE computer interface and IDEAS software provided by Lake Shore. Cooling of the sample was achieved using a closed-cycle cryostat (Advanced Research Systems) and a Lake Shore 340 temperature controller.

3. Results and discussion

The x-ray diffraction pattern of the samples is illustrated in figure 1. X-ray diffractograms of this compound were indexed using the computer program 'Dicvol 04'. The Miller indices (hkl), the observed and calculated interplanar spacings (d), and the relative intensities (I/I_o) of the diffraction lines are listed in table 1. The lattice parameters of the tetragonal unit cell, calculated using the least-squares computer program 'Dicvol 04', were found to be $a = 0.8453(1)$ and $c = 0.6966(5)$ nm. These values are close to the corresponding values reported for $TlInTe_2$ ($a = 0.8494$ and $c = 0.7181$ nm) and $TlGaTe_2$ ($a = 0.8429$ and $c = 0.6865$ nm) crystals [1].

The electrical resistivity (ρ) and Hall coefficient (R_h) of $Tl_2InGaTe_4$ crystals were measured in the temperature region 210–350 K. The sign of the Hall coefficient indicates

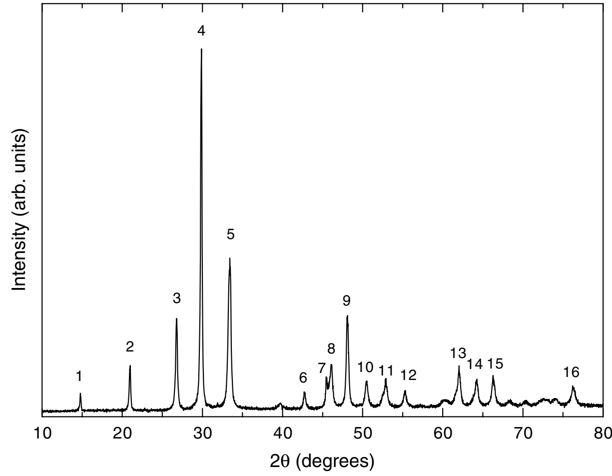

Figure 1. X-ray powder diffraction pattern of $Tl_2InGaTe_4$.

Table 1. X-ray powder diffraction data for $Tl_2InGaTe_4$ crystals.

No.	*h k l*	d_{obs} (nm)	d_{calc} (nm)	I/I_0
1	1 1 0	0.598 85	0.598 84	5
2	2 0 0	0.423 07	0.423 21	12
3	2 1 1	0.332 61	0.332 60	25
4	2 2 0	0.298 97	0.299 13	100
5	3 1 0	0.267 73	0.267 53	37
6	4 0 0	0.211 57	0.211 46	5
7	3 3 0	0.199 35	0.199 36	9
8	4 1 1	0.196 65	0.196 79	10
9	4 2 0	0.189 15	0.189 12	27
10	4 0 2	0.180 77	0.180 77	8
11	3 3 2	0.173 11	0.173 03	8
12	4 2 2	0.166 14	0.166 21	5
13	4 4 0	0.149 47	0.149 49	12
14	5 3 0	0.145 03	0.145 03	8
15	6 0 0	0.140 93	0.140 94	10
16	6 2 2	0.124 83	0.124 82	6

that the crystals exhibit n-type conductivity for all recorded data. The values of the room-temperature electrical resistivity and carrier concentration, $n = (eR_h)^{-1}$, are found to be 2.49×10^3 Ω cm and 4.76×10^{12} cm^{-3}, respectively. The resistivity value reported here coincides with that reported for $TlInTe_2$ crystals, being recorded perpendicular to the *c*-axis [11]. A general view of the electrical resistivity as a function of reciprocal temperature is shown in figure 2. As can be easily detected from the figure, the resistivity sharply increases with decreasing temperature at a nearly constant rate over the whole temperature range that was studied. In particular, ρ increased from 2.14×10^2 Ω cm at 350 K to 4.72×10^6 Ω cm at 210 K. The experimental data of resistivity recorded for $Tl_2InGaTe_4$ crystals are analysed assuming intrinsic-type conduction. The intrinsic electrical resistivity is given by,

$$\rho = \rho_0 \exp\left(\frac{E_g}{2kT}\right), \tag{1}$$

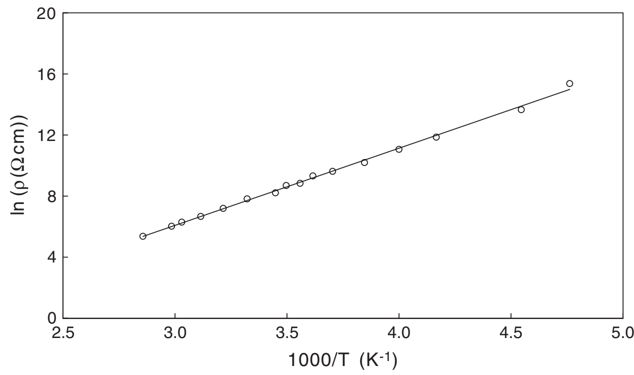

Figure 2. The ρ–T^{-1} variation for $Tl_2InGaTe_4$ crystal. The solid line represents the fit according to equation (1).

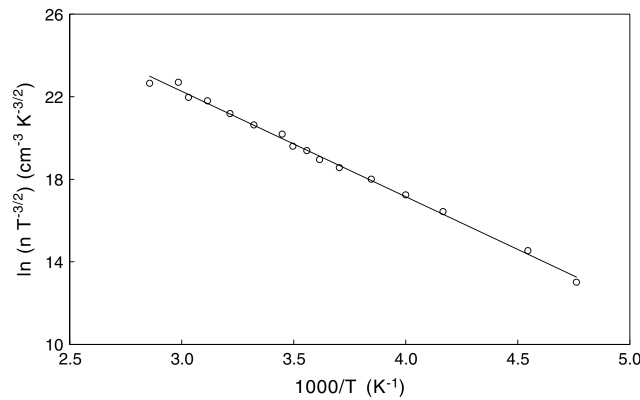

Figure 3. The variation of $\ln(nT^{-3/2})$ versus T^{-1} for $Tl_2InGaTe_4$ crystal. The solid line represents the fit according to equation (2).

where ρ_0 is the pre-exponential factor and E_g is the energy band gap. The experimental data of resistivity was analysed in accordance with equation (1). Plotting $\ln(\rho)$ as a function of reciprocal temperature (T^{-1}) makes the equation linear and reveals a straight line, which in turn gives a slope of $E_g/2k$ (see figure 2). This slope was then used to estimate the energy band gap as 0.85 eV. The obtained band gap confirms the fact that $Tl_2InGaTe_4$ crystals exhibit intrinsic-type conduction and agrees with the electrically and optically determined energy band gaps of 0.80 and 0.97 ($TlInTe_2$) and 0.85 and 0.84 eV ($TlGaTe_2$) crystals [2, 5–7].

It is worth noting that the fitting procedure was carried out using a special high-convergence minimization program that makes use of regression and residual sums of squares (R^2), the coefficient of determination, and residual mean squares statistical analysis. The errors in the data were evaluated to be 2–10%. A typical best fit for the experimental data is illustrated by the solid line in figure 1. The calculated slope was restricted to give a residual sum of squares $R^2 > 0.995$.

To get information about the carrier effective mass in $Tl_2InGaTe_4$ crystals, the temperature dependence of the carrier concentration was analysed in the measured temperature region of 210–350 K. As may be observed from the temperature variation of n shown in figure 3, the carrier concentration strongly decreases from 4.50×10^{13} at 350 K to 1.36×10^{9} cm^{-3} at 210 K, indicating that the crystal exhibits strong compensation. Since the crystal is intrinsic in this temperature range, the experimental carrier density is represented by [16]

$$n = \sqrt{N_c N_v} \exp\left(-\frac{E_g}{2kT}\right) = 4.83 \times 10^{15} (m_c^* m_v^*)^{3/4} T^{3/2} \exp\left(-\frac{E_g}{2kT}\right), \quad (2)$$

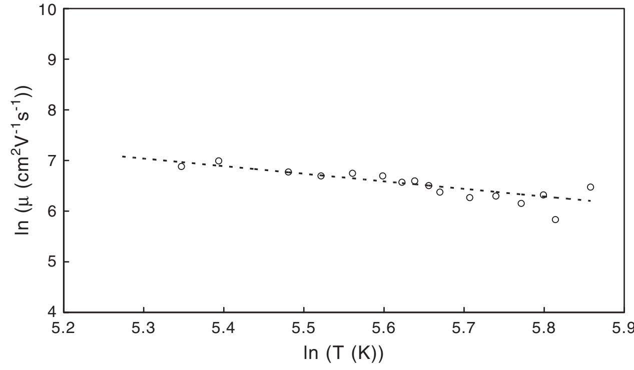

Figure 4. Plot of $\ln(\mu)$–$\ln(T)$ for $Tl_2InGaTe_4$ crystal. The dashed line represents the fit according to equation (3).

where $N_c = 4.83 \times 10^{15}(m_c^* T)^{3/2}$ and $N_v = 4.83 \times 10^{15}(m_v^* T)^{3/2}$ are the effective densities of states in the valence and conduction bands, respectively. Here m_c^* and m_v^* are the carrier effective masses in the conduction and valence bands, respectively. Following the previously reported procedure [16–18] for determining the energy band gap and the carrier's effective mass product and applying equation (2) by plotting $\ln(nT^{-3/2})$ as a function of T^{-1} (see figure 3), the band gap was calculated and found to be 0.85 eV. This value is the same as the value obtained from the resistivity measurement. The intercept of the $\ln(nT^{-3/2})$–T^{-1} plot reveals an effective mass product $(m_c^* m_v^*)$ of $1.62 m_0^2$.

The Hall mobility ($\mu_{exp} = (ne\rho)^{-1}$), calculated from the experimental resistivity and carrier concentration data, exhibits a magnitude of 527 cm^2 V^{-1} s^{-1} at room temperature. The experimental data of Hall mobility as a function of temperature are illustrated in figure 4. The mobility increases with decreasing temperature, reaching the value $\mu = 972$ cm^2 V^{-1} s^{-1} at $T = 210$ K. The slope of logarithmic plot of μ–T is found to be $\sim -3/2$. This value is an indication of the domination of thermal lattice scattering in the crystals. Following our previous works on ternary compounds like $AgIn_5S_8$ [17] and $CuIn_5S_8$ [18] crystals, we attempt to explain the Hall mobility by assuming the domination of acoustic phonons scattering in $Tl_2InGaTe_4$ crystals.

The acoustic phonons' scattering mobility is given by the relation [17–19],

$$\mu_{ac} = 3.17 \times 10^{-5} \frac{du^2}{(m_c^*)^{5/2} E_{ac}^2 T^{3/2}} \text{ cm}^2 \text{ V}^{-1} \text{ s}^{-1}, \quad (3)$$

where d is the density in g cm^{-3}, E_{ac} is the deformation potential in eV for acoustic phonons, and u is the average sound velocity, which could be estimated from the formula,

$$u = \frac{k\theta_D}{\hbar} \left(\frac{V}{6\pi^2} \right)^{1/3} \text{ cm s}^{-1}. \quad (4)$$

Here θ_D is the Debye temperature estimated by Lindemann's melting rule and V is the average atomic volume. In computing the acoustic phonons' scattering mobility, the values of d and V were calculated as 7.40 g cm^{-3} and 4.79×10^{-22} cm^3, respectively, using the x-ray results (reported in the first paragraph of this section) for the $Tl_2InGaTe_4$ crystal. θ_D was estimated as 124 K for a melting temperature of 1045 K. Similar techniques for θ_D estimation were also employed for $AgIn_5S_8$ and $CuIn_5S_8$ crystals, where Debye temperatures of 250 and 226 K, respectively, were reported [17–19].

Unfortunately, the lack of information about the electron's effective mass in the $Tl_2InGaTe_4$ crystals and the experimentally unique observation of intrinsic behaviour of the carrier density (which lead to determination of the $m_c^* m_v^*$ product rather than identification of m_c^* itself) prohibited the determination of the exact value of the acoustic deformation potential. The only available literature data of $m_c^* = 0.35m_o$ (perpendicular to the c-axis) was obtained from band structure studies on $TlInTe_2$ crystal [14], which has the same structural properties as $Tl_2InGaTe_4$ crystal. When $m_c^* = 0.35m_o$ is used to fit the experimental Hall mobility data by means of equation (3), the acoustic deformation potential, which provides a best fit to the experimental data in figure 4, is $E_{ac} = 7.6$ eV. The consistency between the experimentally determined and theoretically evaluated acoustic phonons' scattering mobility data (dashed line) is displayed in figure 4. The dashed line, which represents the theoretical acoustic mobility data obtained from equation (3), fits well to the experimentally determined mobility data at temperatures below 290 K. Above this temperature the experimental data seem to diverge from the theoretical values.

4. Conclusions

In this work we have presented x-ray powder diffraction, resistivity and Hall effect data for $Tl_2InGaTe_4$ crystals at 300 K and in the temperature region 210–350 K, respectively. From the x-ray data the lattice parameters of the tetragonal unit cell, calculated using the least-squares method, were found to be $a = 0.8453(1)$ and $c = 0.6966(5)$ nm. Both resistivity and Hall coefficient analysis have shown that the crystal studied exhibits n-type intrinsic conductivity. The energy band gap of the crystal was calculated to be 0.85 eV. The temperature-dependent carrier concentration and Hall mobility data analysis led to the determination of the conduction and valence bands' carrier effective masses product as $1.62m_0^2$. The Hall mobility is found to be limited by the scattering of acoustic phonons with an acoustic phonon deformation potential of 7.6 eV.

References

[1] Muller D, Eulenberger G and Hahn H 1973 *Z. Anorg. Allg. Chemie* **398** 207
[2] Hanias M, Anagnostopoulos A, Kambas K and Spyridelis J 1989 *Physica* B **160** 154
[3] Hanias M, Anagnostopoulos A, Kambas K and Spyridelis J 1991 *Phys. Rev.* B **43** 4135
[4] Hanias M and Anagnostopoulos A 1993 *Phys. Rev.* B **47** 4261
[5] Nagat A T, Gamal G A and Hussein S A 1990 *Phys. Status Solidi* a **159** K183
[6] Rabinal M K, Titus S S K, Asokan S, Gopal E S R, Godzhaev M O and Mamedov N T 1993 *Phys. Status Solidi* b **178** 403
[7] Abdel-Rahman M 1998 *Indian J. Pure Appl. Phys.* **36** 533
[8] Guseinov G D, Mooser E, Kerimova E M, Gamidov R S, Alekseev I V and Ismailov M Z 1969 *Phys. Status Solidi* **34** 33
[9] Mamedov N T and Moroz N K 1990 *Phys. Status Solidi* b **159** K83
[10] Aliev V I, Aldzhanov M A and Aliev S N 1987 *JETP Lett.* **45** 534
[11] Abdullaev F N, Kerimova T G and Abdullaev N A 2005 *Phys. Solid State* **47** 1221
[12] Orudzhev G S, Godzhaev E M, Kerimova R A and Allakhyarov E A 2006 *Phys. Solid State* **48** 42
[13] Godzhaev E M, Orudzhev G S and Kafarova D M 2004 *Phys. Solid State* **46** 833
[14] Wakita K, Shim Y, Orudzhev G, Mamedov N and Hasimzade F 2006 *Phys. Status Solidi* a **203** 2841
[15] Okazaki K, Tanaka K, Matsuno J, Fujimori A, Mattheiss L F, Iida S, Kerimova E and Mamedov N 2001 *Phys. Rev.* B **64** 045210
[16] Blackmore S K 1962 *Semiconductor Statistics* (New York: Pergamon) p 27
[17] Qasrawi A F and Gasanly N M 2001 *Cryst. Res. Technol.* **36** 457
[18] Qasrawi A F and Gasanly N M 2001 *Cryst. Res. Technol.* **36** 1399
[19] Wiley J D 1975 *Semiconductors and Semimetals* vol 10 (New York: Academic) p 127